

ISSN: (Print) (Online) Journal homepage: www.tandfonline.com/journals/tbsd20

Atranorin, an antimicrobial metabolite from lichen *Parmotrema rampoddense* exhibited in vitro anti-breast cancer activity through interaction with Akt activity

Adhikesavan Harikrishnan, V. Veena, B. Lakshmi, R. Shanmugavalli, Sonia Theres, C. N. Prashantha, Tanya Shah, K. Oshin, Ringu Togam & Sisir Nandi

To cite this article: Adhikesavan Harikrishnan, V. Veena, B. Lakshmi, R. Shanmugavalli, Sonia Theres, C. N. Prashantha, Tanya Shah, K. Oshin, Ringu Togam & Sisir Nandi (2021) Atranorin, an antimicrobial metabolite from lichen *Parmotrema rampoddense* exhibited in vitro anti-breast cancer activity through interaction with Akt activity, Journal of Biomolecular Structure and Dynamics, 39:4, 1248-1258, DOI: [10.1080/07391102.2020.1734482](https://doi.org/10.1080/07391102.2020.1734482)

To link to this article: <https://doi.org/10.1080/07391102.2020.1734482>



View supplementary material [↗](#)



Published online: 09 Mar 2020.



Submit your article to this journal [↗](#)



Article views: 425



View related articles [↗](#)



View Crossmark data [↗](#)



Citing articles: 18 View citing articles [↗](#)



Atranorin, an antimicrobial metabolite from lichen *Parmotrema rampoddense* exhibited in vitro anti-breast cancer activity through interaction with Akt activity

Adhikesavan Harikrishnan^a, V. Veena^b , B. Lakshmi^c, R. Shanmugavalli^a, Sonia Theres^d, C. N. Prashantha^b, Tanya Shah^b , K. Oshin^b, Ringu Togam^b and Sisir Nandi^e

^aDepartment of Chemistry, School of Arts and Sciences, Vinayaka Mission Research Foundation-Aarupadai Veedu (VMRF-AV) Campus, Chennai, Tamil Nadu, India; ^bDepartment of Biotechnology, School of Applied Sciences, REVA University, Bangalore, Karnataka, India; ^cDepartment of Chemistry, School of Applied Sciences, REVA University, Bangalore, Karnataka, India; ^dDepartment of Chemistry, Kanchi Mamunivar Centre for Postgraduate Studies (KMCPGS), Puducherry, India; ^eDepartment of Pharmaceutical Chemistry, Global Institute of Pharmaceutical Education and Research (GIPER), Affiliated to Uttarakhand Technical University, Kashipur, Uttarakhand, India

Communicated by Ramaswamy H. Sarma

ABSTRACT

Atranorin (ATR), lichenized secondary metabolite and depside molecule with several biological potentials such as antimicrobial, anticancer, anti-inflammatory, antinociceptive, wound healing and photo-protective activities. Cytotoxic reports of ATR are documented in several cancer cells and in vivo models but its molecular interaction studies are poorly understood. Therefore, in this present investigation, we have used the in silico studies with biological validation of the molecular targets for the anti-breast cancer mechanism of ATR. The molecular docking studies with the breast cancer oncoproteins such as Bcl-2, Bax, Akt, Bcl-w and Bcl-xL revealed the highest interaction was observed with the Akt followed by Bax, Bcl-xL and Bcl-2 & least with the Bcl-w proteins. The cytotoxicity studies showed ATR selectively inhibited MDA MB-231 and MCF-7 breast cancer cells in differential and dose-dependent manner with the IC₅₀ concentration of 5.36 ± 0.85 μM and 7.55 ± 1.2 μM respectively. Further mechanistic investigations revealed that ATR significantly inhibited ROS production and significantly down-regulated the anti apoptotic Akt than Bcl-2, Bcl-xL and Bcl-w proteins with a significant increase in the Bax level and caspases-3 activity in the breast cancer cells when comparison with Akt inhibitor, ipatasertib. In vitro biological activities well correlated with the molecular interaction data suggesting that atranorin had higher interaction with Akt than Bax and Bcl-2 but weak interaction with Bcl-w and Bcl-xL. In this present study, the first time we report the interactions of atranorin with molecular targets for anti-breast cancer potential. Hence, ATR represents the nature-inspired molecule for pharmacophore moiety for design in targeted therapy.

ARTICLE HISTORY

Received 22 November 2019
Accepted 5 February 2020

KEYWORDS

Breast cancer; interaction; cytotoxicity; atranorin; biological validation

1. Introduction

Breast cancer is the most common cancer among women and the most lethal malignancies. Breast cancer is reported to be the most prevalent and fourth diagnosed cancer in 2008 (Ferlay et al., 2010, Jemal et al., 2010). In breast and prostate cancer, Akt is constantly active or over-expressed due to its own mutations or aberrant activity of upstream proteins of the pathway (Shukla et al., 2020, Paul, Panda, & Thatoi, 2019). Several reports suggested that the inhibition of Akt could reverse its anti-apoptotic processes as well as cellular growth, proliferation and survival of the cancer cells. Reports also suggest that hyperactivation of Akt often increases resistance to chemotherapy or radiotherapy (Hanada, Feng, & Hemmings, 2004). Akt inhibitors have been shown to attenuate this chemotherapeutic resistance when they were administered along with cancer chemotherapy (Bugni et al., 2009, Kizhakkayil

et al., 2010, Shafee, Kaluz, Ru, & Stanbridge, 2009). Research findings have reported that activated Akt protects cancer cells from apoptosis by suppressing NF-κB activity, Bax translocation to mitochondria and caspase-9 cleavage. Caspase-9 has been reported to be directly phosphorylated by activated Akt, and its pro-apoptotic activity being suppressed as a result of this phosphorylation (Wong, Engelman, & Cantley, 2010). An array of reports suggests that the resistance in breast cancer cells to antigrowth stimuli during treatments is attributed to the overexpression of antiapoptotic Bcl-2 family proteins such as Bcl-2, Bcl-xL, and Bcl w (Manero et al., 2006; Zhang et al., 2007). The overexpression of Bcl-2 family proteins not only contributes to the resistance but it is also a major factor for the recurrence of cancer (Kang & Reynolds, 2009, Manero et al., 2006; Zhai et al., 2008). Among the important drivers of cancer, Akt and antiapoptotic Bcl-2 family proteins are vital targets for cancer therapy (Kizhakkayil et al., 2010, Shafee

CONTACT V. Veena  btveenavijaykumar@gmail.com; veena.v@reva.edu.in  Department of Biotechnology, School of Applied Sciences, REVA University, Rukmini Knowledge Park, Kattigenahalli, Yelahanka, Bengaluru, 560064, Karnataka, India

 Supplemental data for this article can be accessed online at <https://doi.org/10.1080/07391102.2020.1734482>.

© 2020 Informa UK Limited, trading as Taylor & Francis Group

et al., 2009, Yang & Wang, 2011). Hence, molecules such targets cancer cell survival, metastasis, inflammation, and induction of apoptosis are of great importance.

ATR is a major constituent reported in many lichens and important members of the depside. Commonly, it is a lichen secondary metabolite reported in several lichens such as *Stereocaulon cacspitorim*, *Everniastrum vexans*, *Parmatrema species* and others (Backorova, Backor, Mikes, Jendzelovsky, & Fedorocko, 2011; Backorova et al., 2012; Neeraj, Behera, Parizadeh, & Bo, 2010; Rajan et al., 2016; Zhou et al., 2017). Biological properties of ATR include antimicrobial agents (Hanada, Feng, & Hemmings, 2004; Pathak, 2017), antinociceptive (Melo et al., 2016; Siqueira et al., 2010), anti-inflammatory (Gargouri et al., 2018), antioxidant (Ristic et al., 2016; Rocha et al., 2010), anticancer (Jeon, Kim, Kim, Youn, & Suh, 2019; Mallavadhani, Somasekhar, Sagarika, & Ramakrishna, 2018; Sahin et al., 2019; Stojanovic et al., 2014) and photoprotective capacity (Ristic et al., 2016; Varol, Tay, Candan, Turk, & Koparal, 2015). An interesting aspect is ATR is a proven non-mutagenic molecule. Also, reports suggest that ATR cream which is patented was able to heal the wound in the male Wistar rats (Barreto et al., 2011; Barreto et al., 2013). More interestingly, the ATR has also reported a non-clastogenic effect on human lymphocytes, which suggests that it is a non-mutagenic compound (Stojanovic et al., 2014). Cytotoxicity of atranorin was reported in various normal and cancer cells of human and animal studies (Dória et al., 2016; Studzinska-Sroka, Galanty, & Bylka, 2017). As per the literature survey, ATR is well-known to exhibit major medicinal benefits. However, the molecular insight of the mode of action is not understood clearly. Our major objective was to identify the target protein against the anti-breast cancer properties of the ATR using the in silico and in vitro approaches.

2. Materials and methods

2.1. In silico studies

2.1.1. Protein identification

Preparation of protein and ligand structures for molecular interaction is being studied. In order to predict the interactions of the atranorin, the target proteins which are highly expressed in the breast cancer cells were used. The sequences of target proteins such as AKT (P31749), BCL-2 (P10415), BAX (Q07812), BCL-W (Q92843) and BCL-XL (CAA80661.1) were retrieved from UniProt Knowledge database. The retrieved sequences were used to predict the template sequences using PSI-BLAST based on the functional domain region of the whole protein available in the protein data bank for the best target selection based on the optimal alignment. The best template sequences after the blast were sorted based on an e-value with >80% of structural similarity. Sequence alignment sheets have been given in the supple document. The resultant template sequences were used to predict the three-dimensional structure using Modeller v.9.12.

2.1.2. Protein preparation

The homology modeling of protein structure is validated using structural analysis and verification server (SAVES v5.0).

Table 1. Protein selection and preparation for docking studies.

Protein	Template	E-value	RMSD	Z-Score	Q-Mean	R Plot	Quality
BCL2	6GL8	0.0	0.10	0.2	0.69	96.1%	85.42%
BAX	4EJN	0.0	0.23	1.2	0.78	98.1%	89.32%
BCL-W	4CIM	0.0	0.12	2.3	0.56	95.0%	100.0%
AKT	4EJN	0.0	0.18	1.1	0.52	96.5%	98.20%
BCL-XL	4QNQ	0.0	0.15	1.36	0.25	96.2%	92.50%

The SAVES tools describe the protein structure with the stereochemical geometry of atoms arranged in 3D protein structure (França TCC 2015; Bhargavi et al., 2010) (Table 1). The Ramachandran plot is predicted to understand the complexity of protein structure with the residue-by-residue geometry optimization and distribution with the 3D structure. Further, to predict the active site amino acids distributed in the modeled protein structure using the CastP calculation server. The CastP calculation helps to predict the active sites based on the calculation of surface area and surface volume within the region of electrostatic, Van der Waals, hydrophobic and hydrophilic interactions of amino acids within the pocket region (Srivastava, Mehta, Sharma, Sharma, & Malik, 2019) (Refer Supplementary file).

2.1.3. Ligand preparation

The structure of ligand, atranorin was retrieved from the PubChem compound database (CID-68066) as described (Jana & Singh, 2019). The pharmacophore modeling and drug-like screening were performed using Molinspiration. The Molinspiration server will calculate the drug-like characters based on Lipinski Rule of 5 such as hydrogen bond donor (<5), hydrogen bond acceptor (<10), Octanol and water dissolution (miLogP <5), molecular weight (<500KDa), number of rotatable bonds (<12) with the selected compounds.

2.1.4. Elucidating the interactions using docking studies

Based on the pharmacophore modeling of ATR were docked with target protein structures using AutoDock4.2. The 3D structure of BCL-2, BCL-XL, BCL-W, AKT, and BAX were used to prepare AutoDock by adding Gasteiger charges, hydrogen atoms were added within polar sites. The ligand structure also prepared with the internal degrees of freedom. The protein torsions were determined to prepare flexible and rigid molecules and to prepare grid maps of different grid points that keep ligands covering binding pockets fully based on active site amino acids within the selected proteins. The grid is prepared within active site amino acid site by adding the grid box by adjusting the x, y and z-axis of 45x45x45 further require to calculate grid parameters using Autogrid. Molecular simulation parameters further to calculate docking properties to understand protein-ligand interaction by adding the Lamarckian Genetic Algorithm was selected with standard docking protocols. Throughout the docking study, the ligand molecules were flexible and macromolecule was kept as rigid. Docking was performed to obtain a population of possible orientations and conformations for the ligand at the binding site (Sanabria-Chanaga, Betancourt-Conde, HernándezCampos, Téllez-Valencia, & Castillo, 2019).

2.2. Biological validation studies

2.2.1. Extraction, purification and structural elucidation of ATR

Parmotrema rampoddense (Nyl.) Hale was collected from Kodaikanal hills, Tamil Nadu, India at an altitude of 1000-1500 m. It was botanically identified by Dr. K.P. Singh, Botanical survey of India, Central circle Allahabad, India. The lichen *Parmotrema rampoddense* material was completely air-dried in the shed and dried lichen (40 g) was crushed grounded to coarse powder form and it was extracted with methanol exhaustively at room temperature. The extracts were filtered and then concentrated under reduced pressure in a rotary evaporator at a temperature of 36 °C. The dried extract (2.5) was fractionated by silica gel (60-120 mesh) column chromatography (60 cm long glass column having a diameter of 6. The adsorbed compound was eluted with benzene followed with benzene-ethyl acetate mixtures, in crescent polarity under a flow rate of 3 ml/min and 39 fractions were collected. The antimicrobial fractions (15-22 tubes) were active against *Bacillus subtilis* and *Staphylococcus aureus*. The active was showing the same Rf values of 0.92 in TLC was performed using system toluene and acetic acid (10: 1.2 v/v) and these were pooled together. The purification of the compound was done by the recrystallization technique using dichloromethane as a solvent for recrystallization. Atranorin was obtained as colorless prismatic rods which weighed around 32 mg and exhibited a sharp melting point of 188-190 °C.

Chemical characterization of the isolated and purified metabolites was performed using UV-Vis, RAMAN spectra, FT-IR and NMR spectroscopic studies. The degree of purity of the lichen compound was > 95% as determined by thin-layer chromatography (TLC), melting point and NMR spectral analyses. UV-Visible spectroscopic results were done using Cary 5E UV-VIS-NIR spectrometer and Methanol was used as the solvent. FT-IR Spectrometer was the model used to record the IR spectrum with a scan range of MIR 450-4000 cm⁻¹ and a resolution of 1.0 cm⁻¹. RAMAN spectral analyses were recorded in BRUKER RFS 27 FT-Raman Spectrometer was the model used to record the Raman spectrum with a scan range of 50-4000 cm⁻¹ and resolution of 2 cm⁻¹. ¹H-NMR analyses were recorded in 500 MHz FT NMR Spectrometer was used to record the ¹H NMR spectrum. Deuterated chloroform (CDCl₃) was used as a solvent. The ¹³C-NMR analysis was recorded using 500 MHz FT NMR Spectrometer was used to record the ¹³C NMR spectrum. ¹³C spectrum of atranorin shows peaks for all the 19 carbon atoms. The chemical shift values for each carbon atom are assigned taking cognizance of the chemical environment of each carbon moiety and the shielding and deshielding effect exhibited by each of the substituents on the respective carbon atom.

2.2.2. In vitro anti-breast cancer studies

Cell lines and maintenance-cancer cell lines (MDA MB-231 and MCF-7) and human embryonic kidney (HEK-293) non-cancer cell lines were obtained from National Centre for Cell Science (NCCS) Pune, India. The cell lines were maintained in DMEM medium supplemented with 10% FBS, 10 U/ml of penicillin, 10 mg/ml of streptomycin, and 0.25 mg/ml of amphotericin-B at 37 °C and 5% CO₂ incubator.

Inhibitory activity of ATR was measured using 3-(4,5 dimethylthiazol-2-yl)-2,5-diphenyl tetrazolium bromide reduction (MTT) assay, as described (Veena, Kennedy, Lakshmi, Krishna, & Sakthivel, 2016). Briefly, cancer cells were seeded at a density of 1 × 10⁵ cells ml⁻¹ in 96 well plates for 24 h in DMEM (200 µl) supplemented with fetal bovine serum (10%). Similarly, non-cancer HEK-293 cells at the same density were used for testing. Different concentrations of ATR (1-50 µM) were treated in octapets and incubated for 48 h at 37 °C in a 5% CO₂ incubator. After treatment, cells were incubated with MTT (10 µl; 5 mg/ml) at 37 °C for 3 h and formazan crystal formed was dissolved in DMSO (100 µl). The plates were read at 590 nm on a scanning multiwell spectrophotometer. The IC₅₀ (concentration of the compound to inhibit 50% on the cells) was obtained by a dose-response curve using the Graph pad prism software of six independent experiments.

2.2.3. Event-based anticancer studies

2.2.3.1. Live dead cell imaging. Cells were cultured in 12-well plates and treated with respective IC₅₀ concentration of atranorin and incubated for 48 h. After incubation, breast cancer cells were stained with AO-EtBr observed under a fluorescent invert microscope for morphological changes.

2.2.3.2 Quantification of cell dead. Cells were cultured in 12-well plates and treated with IC₅₀ concentration of atranorin and incubated for 48 h. After incubation, cells were trypsinized and washed once with PBS. Then, the cells were stained with 200 µl of a mixture (1:1) of acridine orange-ethidium bromide (1 µg/ml) solutions and the cells were counted using the flow cytometer.

2.2.3.3. Generation of ROS. The production of ROS was measured by fluorimetric quantification of fluorescent 2,7-dichlorofluorescein (DCF) formed in the presence of ROS by using cell-permeable non-fluorescent, 2,7-dichlorofluorescein diacetate (DCF-DA). After incubation, the cells were trypsinized, pelleted, washed twice with PBS and exposed to DCF-DA (10 µM) in DMEM medium for 45 min at 37 °C. After incubation, the cells were analyzed using 96-well multimode reader excited at 480 nm and emission was recorded at 540 nm.

2.2.4. Gene expression studies

Total protein from control and treated cells were extracted in the cell lysis buffer at 4 °C. The proteins were stored in -80 °C until the estimation. Caspases-3 activation was measured using caspase-3 (CASP-3F, Sigma) while Akt, Bcl-2 was measured by ELISA (Cayman Chemicals, USA) as per manufacturer instructions.

2.2.5. Statistical studies. The statistical significance of the data was analyzed by the Mann-Whitney U tests with the level of significance, *p* < 0.05 and 95% confidence with the data in octapet of six independent experiments.

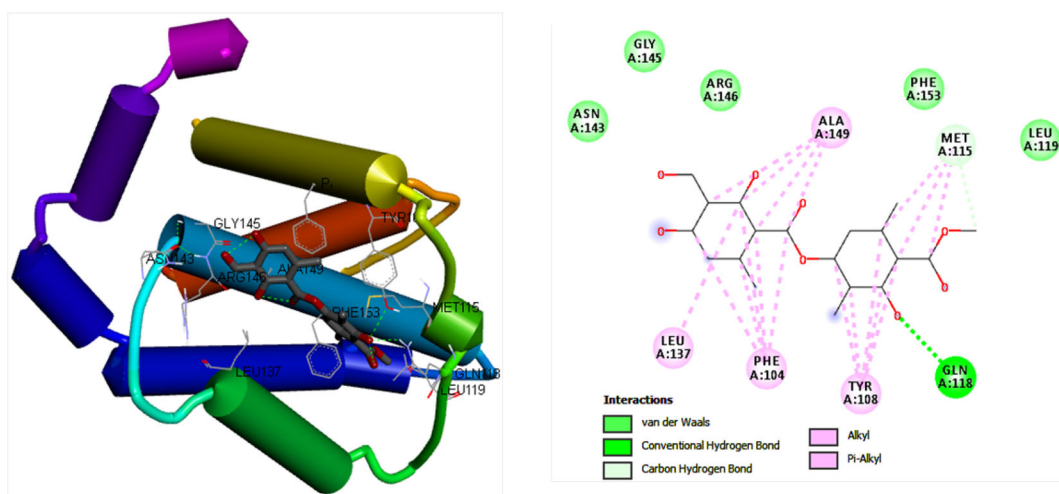


Figure 2. Interaction of ATR with Bcl-2 protein.

Table 3. In silico protein interaction with breast cancer target protein and their interaction

Protein	H-Bonds	Binding Energy	Inhibitory constant	Amino acids
BCL-2	2	-5.58	97.10	Tyr108, Gln118,
BAX	5	-5.42	105.63	Asn73, Glu75, Thr174, Thr182
AKT	4	-7.92	2.61	Leu78, Ser205
BCL-W	5	-4.28	726.97	Leu68, His69, Val70, Thr71, Glu109
BCL-XL	3	-3.18	159.20	Thr118, Ser122, His113

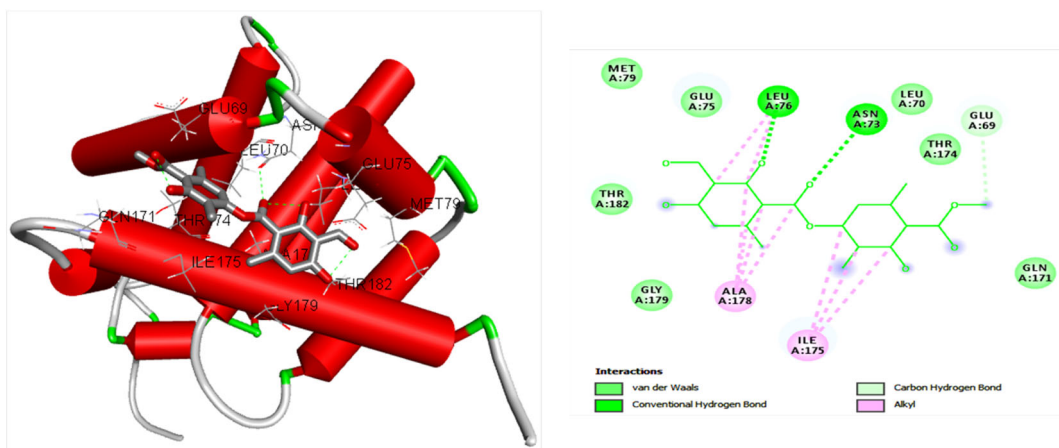


Figure 3. Interaction of ATR with Bax protein.

-4.28 kcal/mol and inhibitory constant was found to be 726.9 μ M. Further, the Bcl-xL - ATR interaction studies showed three hydrogen bonds with the Thr118, Ser122 and His113 with the binding energy of -3.18 kcal/mol and inhibitory constant were found to be 159.20 μ M. According to the in silico studies, the ATR target shows maximum interactions with Akt followed by Bax and Bcl-2. ATR had the least interactions with the Bcl-w and Bcl-xL.

3.2. Extraction, purification and structural identification of ATR

Around 6 g air-dried powder of *Parmotrema rampoddense* (Nyl.) Hale was used for the extraction. The ether extract showed the high inhibitory zone (18 to 22 mm diameter)

against *Bacillus subtilis* and *Staphylococcus aureus* at 1 mg/ml concentration (Mallavadhani et al., 2018; Nasser, Yaacob, Din, Yamin, & Latip, 2009). Further, 2.5 g of the ether extract was used to purify the active metabolites using the column chromatography which yielded 0.065 g of the purified active metabolite identified using the antimicrobial activity assay using a test organism. In the UV-Visible spectrum, the absorption region the aromatic benzene ring normally showed absorption peaks ranging between 230-270nm. The effect of substituents, like the methyl group on the benzene ring, produces a bathochromic shift. The substitution of auxochromic groups like -OH produces a shift to longer wavelengths. The 251.2 nm and 212.6 nm peaks must be due to Ar - CHO and Ar - OH groups respectively.

The FT-IR spectroscopic analyses showed the most important peaks at 2932.6 cm^{-1} denoting chelated -OH group and

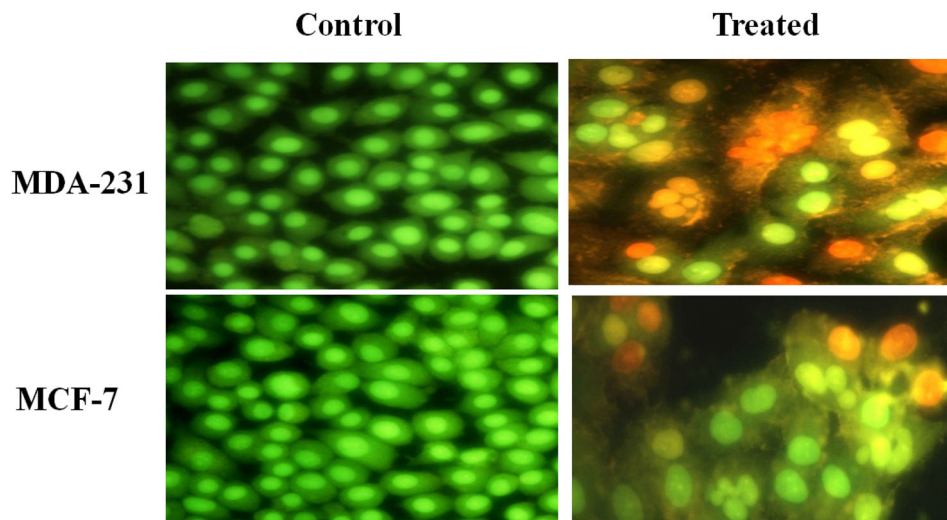


Figure 7. Live dead cell imaging of the breast cancer cells treated with IC50 concentration of ATR at 48 h of exposure.

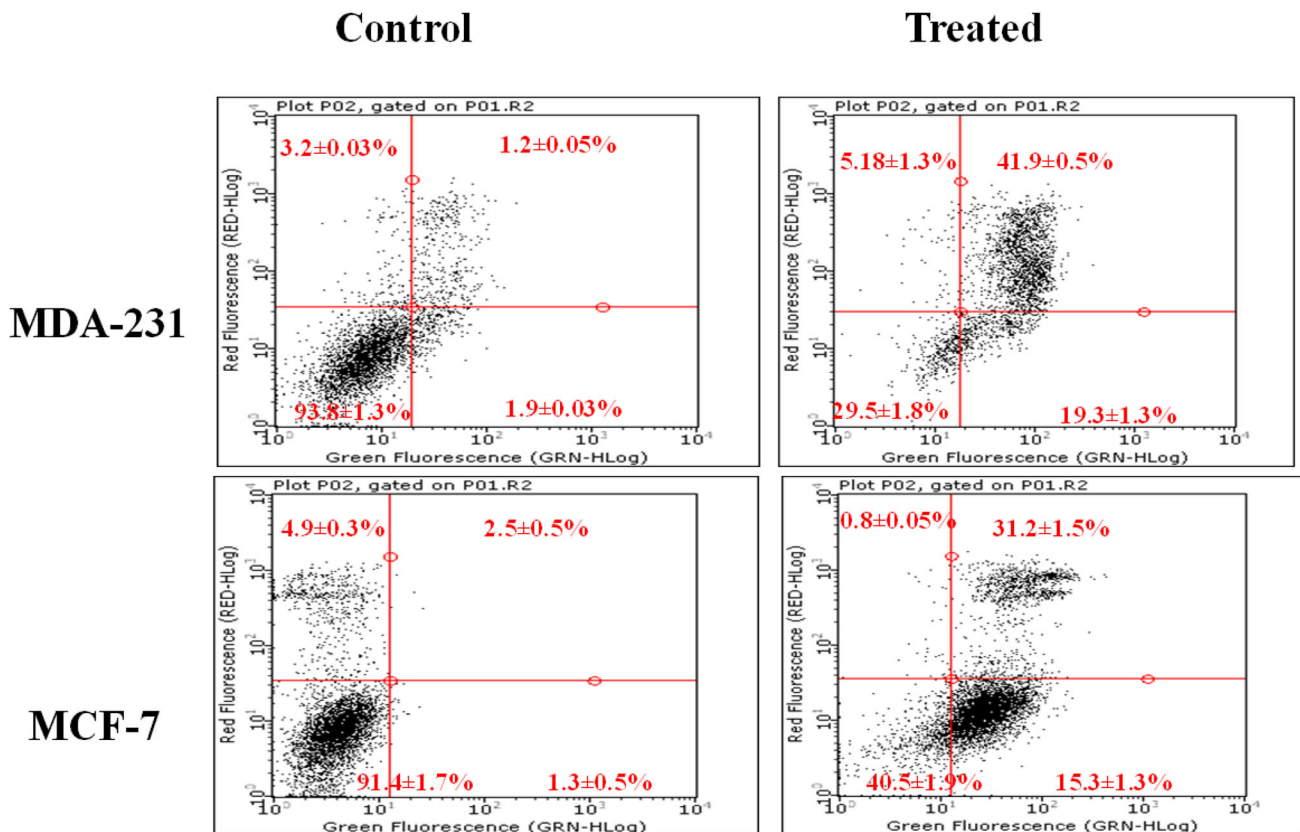


Figure 8. Quantification of cell death by annexin-V FITC and PI staining of the breast cancer cells at 48 h of exposure.

spectrum and NMR spectroscopic method confirmed the identification of the depside atranorin.

3.3. In vitro anti-breast cancer potential of ATR

The cytotoxicity studies showed ATR selectively inhibited breast cancer cells (MDA MB-231 & MCF-7) than the non-cancer cell line (HEK-293) in a differential and dose-dependent manner at 48 h (Figure 6).

The IC₅₀ concentration in MDA MB-231 and MCF-7 cancer cells was found to be $5.36 \pm 0.85 \mu\text{M}$ and $7.55 \pm 1.2 \mu\text{M}$

respectively. This result showed the ATR could inhibit both triple-positive breast cancer (MCF-7) and triple-negative breast cancer (MDA MB-231) cells where the common pathway for these cancers was the over expression of Akt and antiapoptotic Bcl-2 family proteins. These results confirmed the interaction and inhibition of Akt and antiapoptotic Bcl-2 proteins may be the possible inhibitory effect of ATR on breast cancers. Further, normal HEK-293 cells that were not expressing these proteins were not affected. However, the biological outcome of the inhibition may lead to the induction of apoptosis. In order to verify the effect, we performed

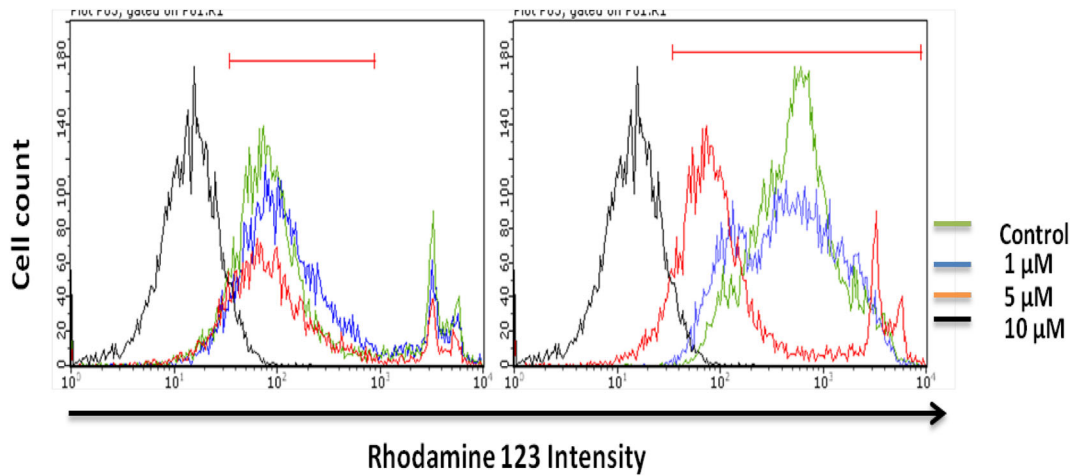


Figure 9. Determination of mitopotential on MCF-7 and MDA MB-231 cells treated with ATR for 48 h of exposure.

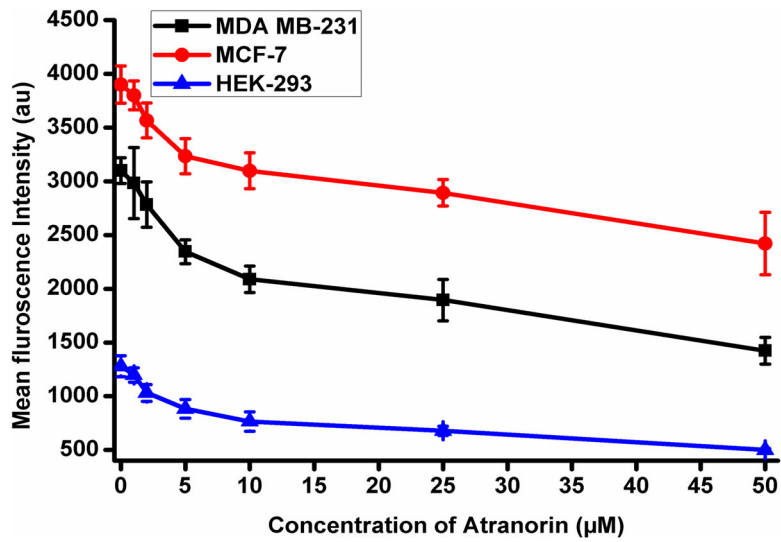


Figure 10. Production of ROS.

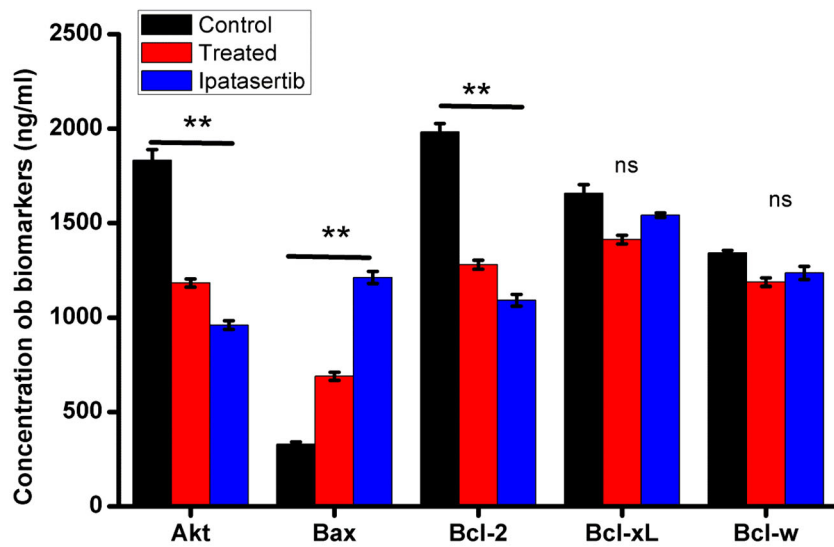


Figure 11. Gene expression studies of ATR (IC₅₀) and ipatasertib (5 μM) on MDA MB-231 cells.

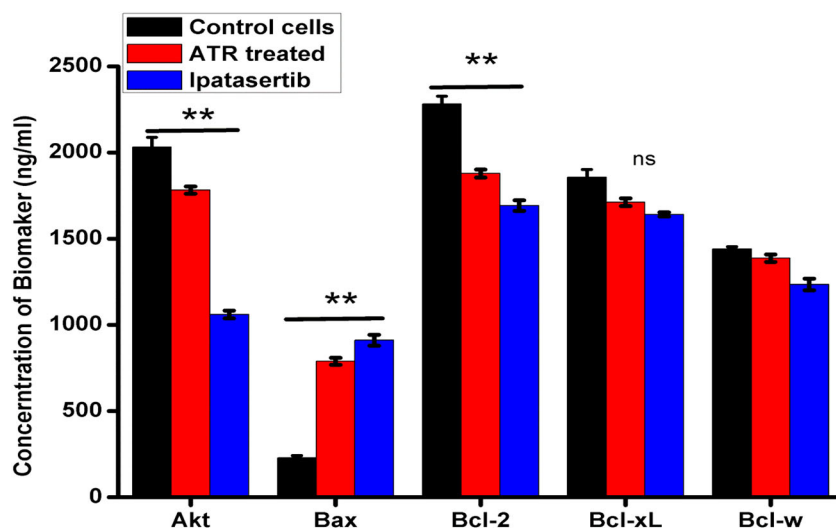


Figure 12. Gene expression studies of ATR (IC_{50}) and ipatasertib ($5 \mu M$) on MCF-7 cells.

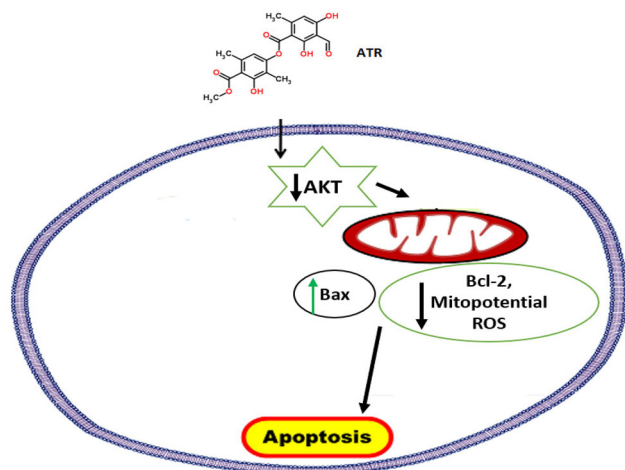


Figure 13. Schematic representation of ATR induced anti-breast cancer activity through induction of mitochondrial mediated pathway through interaction with Akt activity.

the event-based studies and gene expression studies with the respective IC_{50} concentrations in breast cancer cells only.

3.4. Event-based validation of the anti-breast potential of ATR

In order to determine whether ATR induced cell death, we performed AO-EB staining after treatment. The results showed that upon treatment the cell numbers were less, dead cells stained with EB and EB-AO were significantly high when compared to the viable only AO stained cells in control cells (Figure 7).

Further, to quantify the cell death we performed flow cytometric analysis of cell death. The results showed that the presence of early apoptotic cells with $19.3 \pm 1.3\%$ and late apoptotic cell population of $49.9 \pm 0.5\%$ in the MDA MB-231 cells when compared to the control cells that had viable cells of $93.8 \pm 1.3\%$. Similarly, in ATR treated MCF-7 cells the results showed early apoptotic cells were $15.3 \pm 1.3\%$ and

late apoptotic cells were $31.2 \pm 1.5\%$ when compared to control cells with $91.4 \pm 1.7\%$ (Figure 8). These two experimental results confirmed the induction of cell death by ATR in breast cancer cells.

In order to determine the ROS generation and mitopotentiation, we performed CFDA staining and Rhodamine 123 staining respectively. The ROS generation results showed that upon treatment with ATR the mean fluorescent intensity (MFI) was significantly dropped from 3987 ± 76 ($0 \mu M$) to 2897 ± 98 ($50 \mu M$) in MCF-7 cells (Figure 9).

Similarly, in ATR treated MDA MB-231 cells MFI was dropped from 3198 ± 78 ($0 \mu M$) to 1956 ± 56 ($50 \mu M$). These results suggested a reduction in the red-ox potential of the cancer cells. By lowering the red-ox state of breast cancer cells, ATR might induce cell death. This also correlates to the antioxidant potential of the molecule which is popularly reported in the literature.

The mitopotentiation studies through an accumulation of Rh123 dye by the cancer cells showed that $92 \pm 0.7\%$ ($0 \mu M$) population was reduced to the $23.7 \pm 0.2\%$ ($10 \mu M$) in MCF-7 cells and $93.4 \pm 1.2\%$ ($0 \mu M$) population was reduced to the $16.8 \pm 0.7\%$ ($10 \mu M$) in MDA MB-231 cells (Figure 10).

These results suggested that a sharp drop in the mitopotentiation upon ATR treatment might be due to the interaction with the antiapoptotic Bcl-2 family member that resists the cell death via mitochondrial-mediated pathway.

3.5. Gene modulation of the ATR with suspected target proteins

In order to determine the gene expression, we performed ELISA for the oncoproteins such as phosphorylated Akt (p-Akt), Bax, Bcl-2, Bcl-xL, and Bcl-W from the protein extracted after treatment with the respective IC_{50} concentrations of ATR (Figures 11 and 12).

The results showed the maximum significant downregulation of p-Akt followed by Bcl-2, then Bax, and no signs were observed in the Bcl-W and Bcl-xL in both cell lines. Ipatasertib, a standard control for Akt, was used as a positive

control (Srivastava et al., 2019). These in vitro results correlated with the in silico studies. Hence, we report that ATR induced anti-breast cancer activity through inhibition of the Akt via induction of mitochondrial mediated apoptotic pathway (Figure 13)

4. Conclusion

The combined in silico and in vitro approaches reveal that ATR to be potential natural ligand with the multi targets for several biological outcomes. From our present investigations, we conclude that ATR which was purified from *Parmotrema rampoddense* exhibited anti-breast cancer potential may be a potent inhibitor for Akt and antiapoptotic Bcl-2 family proteins. Among the proteins, ATR had a high affinity to Akt but could have only four hydrogen bonds with two important amino acids at the allosteric of the Akt protein only that regulates the functionality of the protein. The next protein was Bax, where ATR can occupy the BH3 domain with five hydrogen bonds of four amino acids where the anti apoptotic Bcl-2 proteins bind and inhibit apoptosis. While ATR had weak inhibition of interactions with Bcl-2, Bcl-xL and Bcl-W proteins. However, the detailed in vitro analyses showed the process of downregulation of oncoproteins specific to breast cancer to inhibit the proliferation and progression of breast cancer cells. The in silico studies correlates with the in vitro gene expression studies of breast cancer model leading to the induction of apoptosis in the breast cancer cells is the major outcome of the ATR-Akt interactions. These onco proteins of breast cancer are the major targets in the inflammation, cancer and cancer-related inflammations. These interactions and interacting groups of ATR to targets of cancer-related inflammations makes the molecule that could be further used to develop the NSAIDs for breast cancer. This study also provides the future pharmacological natural backbone for targeted therapy in cancer treatment. Hence, further investigation and in vivo studies could be efficient as anticancer molecules based on the pharmacophore moiety of ATR as nature-inspired anticancer molecules.

Disclosure statement

No potential conflict of interest was reported by the authors.

ORCID

V. Veena  <http://orcid.org/0000-0001-9439-639X>

Tanya Shah  <http://orcid.org/0000-0002-9787-522X>

References

- Backorova, M., Backor, M., Mikes, J., Jendzelovsky, R., & Fedorocko, P. (2011). Variable responses of different human cancer cells to the lichen compounds parietin, atranorin, usnic acid and gyrophoric acid. *Toxicology in Vitro*, 25, 37–44.
- Backorova, M., Jendzelovsky, R., Kello, M., Backor, M., Mikes, J., & Fedorocko, P. (2012). Lichen secondary metabolites are responsible for induction of apoptosis in HT-29 and A2780 human cancer cell lines. *Toxicology in Vitro*, 26, 462–468. doi:10.1016/j.tiv.2012.01.017
- Barreto, R., Albuquerque-Júnior, R., Pereira-Filho, R. N., Quintans, J., Barreto, A. S., DeSantana, J. M., ... Quintans-Júnior, L. J. (2013). Evaluation of wound healing activity of Atranorin, a lichen secondary metabolite, on rodents. *Revista Brasileira de Farmacognosia*, 23(2), 310–319. doi:10.1590/S0102-695X2013005000010
- Barreto, R. S., Araújo, B., Siqueira, J. S., DeSantana, J. M., Araújo, A., Barreto, A. S., & Santos, M. (2011). Bioassay-guided evaluation of wound healing effect of atranorin in rodents. *Federation of American Societies for Experimental Biology Journal*, 25, 1.
- Bhargavi, K., Chaitanya, P. K., Ramasree, D., Vasavi, M., Murthy, D. K., & Uma, V. (2010). Homology Modeling and Docking Studies of Human Bcl-2L10 Protein. *Journal of Biomolecular Structure and Dynamics*, 28(3), 379–391. doi:10.1080/07391102.2010.10507367
- Bugni, T. S., Andjelic, C. D., Pole, A. R., Rai, P., Ireland, C. M., & Barrows, L. R. (2009). Biologically active components of a Papua New Guinea analgesic and anti-inflammatory lichen preparation. *Fitoterapia*, 80 (5), 270–273. doi:10.1016/j.fitote.2009.03.003
- Dória, A., Menezes, P. P., Lim, B. S., Vasconcelos, B. S., Silva, F., de Sergipe, F., ... de Sergipe, F. (2016). In vivo antitumor effect, induction of apoptosis and safety of *Remirea maritima* Aubl. (Cyperaceae) extracts. *Phytomedicine*, 23 (9), 914–922. doi:10.1016/j.phymed.2016.05.001
- Ferlay, J., Shin, H.-R., Bray, F., Forman, D., Mathers, C., & Parkin, D. M. (2010). Estimates of worldwide burden of cancer in 2008: GLOBOCAN 2008. *International Journal of Cancer*, 127(12), 2893–2917. doi:10.1002/ijc.25516
- França, T. (2015). Homology modeling: An important tool for the drug discovery. *Journal of Biomolecular Structure and Dynamics*, 33(8), 1780–1793. doi:10.1080/07391102.2014.971429
- Fratev, F., Gutierrez, D. A., Aguilera, R. J., Tyagi, A., Damodaran, C., & Sirimulla, S. (2020). Discovery of New AKT1 Inhibitors by combination of in silico structure based virtual screening approaches and biological evaluations. *Journal of Biomolecular Structure and Dynamics*, 1–10. doi:10.1080/07391102.2020.1715835
- Gargouri, B., Carstensen, J., Bhatia, H. S., Huell, M., Dietz, G. P. H., & Fiebich, B. L. (2018). Anti-neuroinflammatory effects of Ginkgo biloba extract EGb761 in LPS-activated primary microglial cells. *Phytomedicine*, 44, 45–55. doi:10.1016/j.phymed.2018.04.009
- Hanada, M., Feng, J., & Hemmings, B. A. (2004). Structure, regulation and function of PKB/AKT—a major therapeutic target. *Biochimica et Biophysica Acta (Bba) - Proteins and Proteomics*, 1697 (1–2), 3–16. doi:10.1016/j.bbapap.2003.11.009
- Jana, S., & Singh, S. K. (2019). Identification of selective MMP-9 inhibitors through multiple e-pharmacophore, ligand-based pharmacophore, molecular docking, and density functional theory approaches. *Journal of Biomolecular Structure and Dynamics*, 37(4), 944–965. doi:10.1080/07391102.2018.1444510
- Jemal, A., Bray, F., Center, M. M., Ferlay, J., Ward, E., & Forman, D. (2010). Global cancer statistics CA Cancer Journal for Clinicians, 61, 69–90. doi:10.3322/caac.20107
- Jeon, Y., Kim, S., Kim, J. H., Youn, U. J., & Suh, S. (2019). The Comprehensive Roles of Atranorin, a Secondary Metabolite from the Antarctic Lichen *Stereocaulon caespitosum*, in HCC Tumorigenesis. *Molecules*, 24, 1414. doi:10.3390/molecules24071414
- Kang, M. H., & Reynolds, C. P. (2009). Bcl-2 Inhibitors: Targeting mitochondrial apoptotic pathways in cancer therapy. *Clinical Cancer Research*, 15(4), 1126–1132. doi:10.1158/1078-0432.CCR-08-0144
- Kizhakkayil, J., Thayyullathil, F., Chathoth, S., Hago, A., Patel, M., & Galadari, S. (2010). Modulation of curcumin-induced Akt phosphorylation and apoptosis by PI3K inhibitor in MCF-7 cells. *Biochemical and Biophysical Research Communications*, 394 (3), 476–481. doi:10.1016/j.bbrc.2010.01.132
- Lakshmi, P., Kumar, A., Veena, V., Sakthivel, N., & Krishna, R. (2017). Identification of Natural Allosteric Inhibitor for Akt1 Protein through Computational Approaches and in vitro Evaluation. *International Journal of Biological Macromolecules*, 96, 200–213. doi:10.1016/j.ijbiomac.2016.12.025
- Mallavadhani, U. V., Somasekhar, T., Sagarika, G., & Ramakrishna, S. (2018). Isolation, chemical modification and cytotoxic evaluation of atranorin, the major metabolite of the foliose lichen *Parmotrema*

- Melanothrix*. *European Chemical Bulletin*, 7(4-6), 150–155. doi:10.17628/ecb.2018.7.150-155
- Manero, F., Gautier, F., Gallenne, T., Cauquil, N., Grée, D., Cartron, P.-F., ... Juin, P. (2006). The small organic compound HA14-1 prevents Bcl-2 interaction with Bax to sensitize malignant glioma cells to induction of cell death. *Cancer Research*, 66(5), 2757–2764. doi:10.1158/0008-5472.CAN-05-2097
- Mayan, K., Samarakoon, S. R., Tennekoon, K. H., Siriwardana, A., & Valverde, J. R. (2016). Evaluation of Selected Natural Compounds for Cancer Stem Cells Targeted Anti-cancer Activity: A Molecular Docking Study. *European Journal of Medicinal Plants*, 15(4), 1–21. doi:10.9734/EJMP/2016/27847
- Melo, M., Santosh, P. A., Serafini, M. R., Caregnato, F. F., Pasquali, M., Rabelo, T. K., ... Vila, J. L. (2016). Presence of Atranorin in *Physcia Sorediosa*. *Bolivian Journal of Chemistry*, 33(5), 174–178.
- Nasser, J. A., Yaacob, W. A., Din, L. B., Yamin, B. M., & Latip, J. (2009). Isolation of atranorin, bergenin and goniothalamin from *hopea sangal*. *ARPN Journal of Engineering and Applied Sciences*, 4(1), 1.
- Neeraj, V., Behera, B., Parizadeh, H., & Bo, S. (2010). Bactericidal Activity of Some Lichen Secondary Compounds of *Cladonia ochrochlora*, *Parmotrema nilgherrensis* & *Parmotrema sancti-angelii*. *International Journal of Drug Development & Research*, 3 (3), 222–232.
- Pathak, A. (2017). Virtual Docking analysis of Atranorin with Fungal Class I Hydrophobin. *Research Journal of Life Sciences, Bioinformatics, Pharmaceutical and Chemical Sciences*, 3(3), 242.
- Paul, M., Panda, M. K., & Thatoi, H. (2019). Developing Hispolon-based novel anticancer therapeutics against human (NF- κ B) using in silico approach of modelling, docking and protein dynamics. *Journal of Biomolecular Structure and Dynamics*, 37(15), 3947–3967. doi:10.1080/07391102.2018.1532321
- Rajan, V. P., Gunasekaran, S., Ramanathan, S., Murugaiyah, V., Samsudin, M. W., & Din, L. B. (2016). Biological activities of four *Parmotrema* species of Malaysian origin and their chemical constituents. *Journal of Applied Pharmaceutical Science*, 6 (08), 036–043. doi:10.7324/JAPS.2016.60806
- Ristic, S., Rankovic, B., Kosanic, M., Stanojkovic, T., Stamenkovic, S., Vasiljevic, P., ... Manojlovic, N. (2016). Phytochemical study and antioxidant, antimicrobial and anticancer activities of *Melanelia subaurifera* and *Melanelia fuliginosa* lichen. *Journal of Food Science and Technology*, 53(6), 2804–2816.
- Rocha, R. F., Quintans, L. R., Jr Araujo, A. S., Silva, F. A., Moreira, J. C. F., & Gelain, D. P. (2010). Redox properties and cytoprotective actions of atranorin, a lichen secondary metabolite. *Toxicology in Vitro*, 25, 462–468. doi:10.1016/j.tiv.2010.11.014
- Sahin, E., Psav, S. D., Avan, I., Candan, M., Sahinturk, V., & Kopalal, A. T. (2019). Cytotoxic, apoptotic and cell migration inhibitory effects of atranorin on SPC212 mesothelioma cells. *Asian Pacific Journal of Tropical Biomedicine*, 9(7), 299–306. doi:10.4103/2221-1691.261810
- Sanabria-Chanaga, E. E., Betancourt-Conde, I., HernándezCampos, A., Téllez-Valencia, A., & Castillo, R. (2019). In silico hit optimization toward AKT inhibition: Fragment-based approach, molecular docking and molecular dynamics study. *Journal of Biomolecular Structure and Dynamics*, 37(16), 4301–4431. doi:10.1080/07391102.2018.1546618
- Shafee, N., Kaluz, S., Ru, N., & Stanbridge, E. J. (2009). PI3K/Akt activity has variable cell-specific effects on expression of HIF target genes, CA9 and VEGF, in human cancer cell lines. *Cancer Letters*, 282 (1), 109–115. doi:10.1016/j.canlet.2009.03.004
- Shukla, A., Tyagi, R., Meena, S., Datta, D., Srivastava, S. K., & Khan, F. (2020). 2D- and 3D-QSAR modelling, molecular docking and in vitro evaluation studies on 18 β -glycyrrhetic acid derivatives against triple-negative breast cancer cell line. *Journal of Biomolecular Structure and Dynamics*, 38(1), 168–185. doi:10.1080/07391102.2019.1570868
- Siqueiraa, R. S., Bonjardima, L. R., Araújo, A., Araújo, B., Melo, M., Oliveiraa, M., ... Quintans-Júniora, L. J. (2010). Antinociceptive Activity of Atranorin in Mice Orofacial Nociception Tests. *Journal of Natural Science Tubingen*, 65, 551–561.
- Srivastava, S., Mehta, P., Sharma, O., Sharma, M., & Malik, R. (2019). Computationally guided identification of Akt-3, a serine/threonine kinase inhibitors: Insights from homology modelling, structure-based screening, molecular dynamics and quantum mechanical calculations. *Journal of Biomolecular Structure and Dynamics*, 1–10. doi:10.1080/07391102.2019.1675536
- Stojanovic, G. S., Stankovic, M., Stojanovic, I. Z., Palic, I., Milovanovic, V., & Rancic, S. (2014). Clastogenic effect of atranorin, evernic acid, and usnic acid on human lymphocytes. *Natural Product Communications*, 9(4), 503–504.
- Studzinska-Sroka, E., Galanty, A., & Bylka, W. (2017). Atranorin-An Interesting Lichen Secondary Metabolite. *Mini-Reviews in Medicinal Chemistry*, 17 (17), 1633–1645. doi:10.2174/1389557517666170425105727
- Trejo-Soto, P. J., Hernández-Campos, A., Romo-Mancillas, A., Medina-Franco, J. L., & Castillo, R. (2018). In search of AKT kinase inhibitors as anticancer agents: Structure-based design, docking, and molecular dynamics studies of 2,4,6-trisubstituted pyridines. *Journal of Biomolecular Structure and Dynamics*, 36(2), 423–442. doi:10.1080/07391102.2017.1285724
- Varol, M., Tay, T., Candan, M., Turk, A., & Kopalal, A. (2015). Evaluation of the sunscreen lichen substances usnic acid and atranorin. *BIOCELL*, 39(1), 25–31.
- Veena, V., Kennedy, R. K., Lakshmi, P., Krishna, R., & Sakthivel, N. (2016). Anti-leukemic, anti-lung and anti-breast cancer potential of the microbial polyketide, 2,4-diacetylphloroglucinol (DAPG) and its interaction with the metastatic proteins than the antiapoptotic Bcl-2 proteins. *Molecular and Cellular Biochemistry*, 414 (1-2), 47–56. doi:10.1007/s11010-016-2657-6
- Wong, K., Engelman, J. A., & Cantley, L. C. (2010). Targeting the PI3K signaling pathway in cancer. *Current Opinion in Genetics & Development*, 20, 87–90. doi:10.1016/j.gde.2009.11.002
- Yang, C., & Wang, S. (2011). Hydrophobic binding hot spots of Bcl-xL protein–protein interfaces by cosolvent molecular dynamics simulation. *ACS Medicinal Chemistry Letters*, 2 (4), 280–284. doi:10.1021/ml100276b
- Zhai, D., Jin, C., Shiao, C., Kitada, S., Satterthwait, A. C., & Reed, J. C. (2008). Gambogic acid is an antagonist of antiapoptotic Bcl-2 family proteins. *Molecular Cancer Therapeutics*, 7(6), 1639–1646. doi:10.1158/1535-7163.MCT-07-2373
- Zhang, M., Ling, Y., Yang, C.-Y., Liu, H., Wang, R., Wu, X., ... Yang, D. (2007). A novel Bcl-2 small molecule inhibitor 4-(3-methoxy-phenylsulfanyl)-7-nitro-benzofurazan-3-oxide(MNB)-induced apoptosis in leukemia cells. *Annals of Hematology*, 86 (7), 471–481. doi:10.1007/s00277-007-0288-4
- Zhang, L., Ming, L., & Yu, J. (2007). BH3 mimetics to improve cancer therapy; mechanisms and examples. *Drug Resistance Updates*, 10 (6), 207–217. doi:10.1016/j.drug.2007.08.002
- Zhou, R., Yang, Y., Park, S., Nguyen, T. T., Seo, Y., Lee, K. H., ... Kim, H. (2017). The lichen secondary metabolite atranorin suppresses lung cancer cell motility and tumorigenesis. *Scientific Reports*, 7(1), 8136. doi:10.1038/s41598-017-08225-1